



HAL
open science

Dust iron dissolution in seawater: Results from a one-year time-series in the Mediterranean Sea

Thibaut Wagener, Elvira Pulido-Villena, Cécile Guieu

► To cite this version:

Thibaut Wagener, Elvira Pulido-Villena, Cécile Guieu. Dust iron dissolution in seawater: Results from a one-year time-series in the Mediterranean Sea. *Geophysical Research Letters*, 2008, 35 (16), pp.L16601. 10.1029/2008GL034581 . hal-02567417

HAL Id: hal-02567417

<https://hal.science/hal-02567417v1>

Submitted on 27 Oct 2020

HAL is a multi-disciplinary open access archive for the deposit and dissemination of scientific research documents, whether they are published or not. The documents may come from teaching and research institutions in France or abroad, or from public or private research centers.

L'archive ouverte pluridisciplinaire **HAL**, est destinée au dépôt et à la diffusion de documents scientifiques de niveau recherche, publiés ou non, émanant des établissements d'enseignement et de recherche français ou étrangers, des laboratoires publics ou privés.

Dust iron dissolution in seawater: Results from a one-year time-series in the Mediterranean Sea

Thibaut Wagener,¹ Elvira Pulido-Villena,¹ and Cécile Guieu¹

Received 5 May 2008; revised 19 June 2008; accepted 27 June 2008; published 19 August 2008.

[1] A better comprehension of atmospheric iron dissolution in seawater would be a key advance in understanding the atmospheric supply of iron to the ocean and its role on marine biogeochemistry. So far, different studies have demonstrated that dissolution of atmospheric iron depends on physical and chemical properties of the particles, which can be modified during their transport from the source. Here, based on a one-year time-series in the Western Mediterranean Sea, we show that dissolution of iron from a Saharan desert dust sample in seawater follows the seasonal trend of the dissolved organic carbon (DOC) variability in the surface layer. As part of the DOC pool, the role of iron binding ligands, probably derived from bacteria activity, has also been investigated. The dust iron dissolution rates are found to be linearly dependent on iron binding ligands and dissolved organic carbon concentrations ($r^2 > 0.65$, $p < 0.01$, $n = 9$). **Citation:** Wagener, T., E. Pulido-Villena, and C. Guieu (2008), Dust iron dissolution in seawater: Results from a one-year time-series in the Mediterranean Sea, *Geophys. Res. Lett.*, *35*, L16601, doi:10.1029/2008GL034581.

1. Introduction

[2] At the end of the 80's, two new concepts brought an important focus on iron biogeochemistry within the coupled ocean-atmosphere system: (1) iron limits oceanic productivity in the large High Nutrient Low Chlorophyll (HNLC) areas and (2) atmospheric particles (in particular desert dust) are the main external source of iron for the open ocean. The 'iron hypothesis' expressed by *Martin* [1990] linked these two concepts over long time-scales. One of the keys for improving the comprehension and quantification of this link is a better understanding/parameterization of the dissolution of iron from atmospheric deposition into the sea surface waters.

[3] The influence of chemical and physical properties of atmospheric particles, and their aging during atmospheric transport towards iron dissolution in water has been investigated in previous studies [e.g., *Baker and Jickells*, 2006; *Sedwick et al.*, 2007]. At the seawater pH ($\text{pH} \sim 8$), the solubility of iron (III) is extremely low, but is enhanced by organic binding ligands [*Liu and Millero*, 2002]. Ligands have been demonstrated to be in excess compared to dissolved iron and to form strong iron-complexes ($K_{\text{cond}}\text{Fe}^{\text{L}} \sim 10^{12}$) [*Van den Berg*, 1995]. Several experimental studies have pointed out that "natural strong iron binding ligands" enhance the dissolution of iron (hydr)oxides in aquatic systems [e.g., *Kraemer*, 2004]. Iron binding ligands com-

pose a part of the complex dissolved organic matter (DOM) pool, whose content in seawater is related to the biogeochemical conditions. Since biogeochemical conditions exhibit seasonal variations, it is likely that the dissolution of atmospheric iron varies accordingly.

[4] The aim of this study is to investigate the influence of ocean biogeochemistry on dust iron dissolution rather than to provide absolute values for dissolution. It has to be seen as complementary to previous studies that have focused mainly on the influence of the aerosol physical and chemical properties toward the dissolution and "effective" dissolution estimates made in surface seawater [e.g., *Sedwick et al.*, 2007].

2. Material and Methods

2.1. Sampling and Analysis

[5] Seawater sampling was performed monthly between December 2005 and December 2006 at the JGOFS-DYFAMED time-series station ($43^{\circ}25'N$, $07^{\circ}52'E$). Seawater was collected on board the R/V *Tethys II* at a 10 m depth using a trace metal clean protocol described by *Bonnet and Guieu* [2006]. This water mass is representative of the oceanic surface layer impacted by atmospheric deposition. Filtered seawater ($<0.2\mu\text{m}$ –Sartobran cartridge filter) was collected for measurements of dissolved iron concentration [dFe], dissolved organic carbon concentration (DOC) and excess iron binding ligands concentration (cf. Introduction) [L']. Additional filtered seawater was sampled to perform dissolution experiments. Bulk samples were collected for bacterial abundance (BA). Samples for the dissolution experiments and [L'] determination were immediately deep-frozen (-20°C) on board until the experiments or analyses were performed. The rest of the samples were kept at 4°C .

[6] [dFe] was analyzed by flow injection with online pre concentration and chemiluminescence detection following exactly the same protocol and analytical parameters as *Bonnet and Guieu* [2006] (detection Limit (DL) = 10 pM and blank = 50 pM, same instrument used). All filtered samples for [dFe] determinations were acidified (0.01M HCl - Merck Ultrapur) at least 24 hours before analysis. DOC was determined with a Shimadzu TOC analyzer and BA was determined by epifluorescence microscopy (both described by *Pulido-Villena et al.* [2008]). [L'] was determined by a competitive ligand equilibration with 2-(2-thiazolyazo)-p-cresol (TAC) followed by adsorptive cathodic stripping voltammetry (CL-ACSV) [*Croot and Johansson*, 2000]. [L'] were calculated with the "Van den Berg/Ruzic" linearization method considering only one class of ligands (see auxiliary material¹).

¹Laboratoire d'Océanographie de Villefranche, UMR7093, CNRS, Villefranche-sur-Mer, France.

2.2. Dissolution Experiments

[7] The fraction $<20 \mu\text{m}$ of a soil composite collected in the South Algerian Hoggar Region (hereafter “dust”) with iron concentration of $5\% \pm 0.5\%$ in mass, was used for the two dissolution experiments. This material has been used in various studies, as a proxy for aerosol samples. Although this material has not been subject to atmospheric transport, its grain-size distribution is representative of dust transported over the western Mediterranean Sea [Guieu *et al.*, 2002]. The first experiment was devoted to assess the seasonal variability of iron dissolution; the second one was devoted to investigate the iron dissolution kinetics. All manipulations took place under a class 100 laminar flow bench and all material was cleaned following trace-metal clean protocols.

[8] The first dissolution experiment was performed by adding a fixed amount of the same dust to seawater collected at 10 different moments of the year at the DYFAMED site. Seawater was defrosted the evening before the experiment. In a small Teflon vial, 10 mL of Milli-Q water was added to 10 mg of dust and vigorously shaken. 1 mL of this “mother solution” was immediately added into 200 mL of seawater (final dust concentration = $5 \text{ mg}\cdot\text{L}^{-1}$) and the bottles were vigorously shaken. 60 mL were immediately filtered on a $0.2 \mu\text{m}$ polycarbonate membrane for the measurement of [dFe]. This represents the time T_{insta} and occurred after *ca.* 120 s. Bottles with the remaining $5 \text{ mg}\cdot\text{L}^{-1}$ dust solution were shaken every 4 to 8 hours. After 24 hours (T_{24}) and 72 hours (T_{72}), 60 mL were filtered under the same conditions as for T_{insta} for the measurements of [dFe].

[9] For the second experiment, a “seawater composite” was obtained by mixing together an equal amount of the 10 filtered seawaters used in the first experiment. The experiment was performed in duplicate and was designed to parameterize the iron dissolution kinetics. For both replicates, 5 mg of dust was added to 1 L of seawater (final dust concentration: $5 \text{ mg}\cdot\text{L}^{-1}$). 60 mL of the seawater/dust solution were filtered on a $0.2 \mu\text{m}$ membrane for [dFe] determinations at the following 15 times: 1, 5, 15, 30 min and 1, 2, 4, 8, 12, 16, 24, 48, 72, 96, 120h. Between filtrations, the two containers were placed on a shaker (frequency: 1 s^{-1}). It has to be mentioned that the final dust concentration used in this experiment is higher than that expected in the surface mixed layer after most typical-intensity Saharan events in the Mediterranean Sea (see range proposed by Bonnet and Guieu [2004]).

[10] Wall adsorption of iron can be an issue in such experiments [Fischer *et al.*, 2007] and organic matter coagulation could have biased the interpretation of the results; however, all the experiments having been conducted under the same conditions, we assume that comparing the results of these experiments is a valuable exercise.

3. Results

3.1. Temporal Variations of Seawater Biogeochemical Conditions

[11] [dFe] averaged 0.6 nM during the winter mixing period, followed by a decrease to 0.2 nM at the end of the spring bloom in May (Figure 1b). [dFe] then increased to

1.5 nM during the stratification period. [L'] were always in excess compared to [dFe] with higher values during spring and summer (May to August) compared to winter and fall (Figure 1a). DOC and BA followed synchronous trends with low values from October to April, increasing in May after the end of the spring bloom (Figures 1c and 1d). TChla indicated the occurrence of a significant spring bloom (TChla = $2.5 \mu\text{g}\cdot\text{L}^{-1}$) at the end of March. Summer values were typical of oligotrophic conditions ($0.02 < \text{TChla} < 0.05 \mu\text{g}\cdot\text{L}^{-1}$, Figure 1e).

3.2. Seasonal Variability of Atmospheric Iron Dissolution (First Experiment)

[12] [dFe] released from particles ($\Delta[\text{dFe}]$ in nM) at T_{insta} was undetectable (DL for $\Delta[\text{dFe}]$ being 0.01 nM). $\Delta[\text{dFe}]$ at T_{24} ranged from $<\text{DL}$ to 0.26 nM and at T_{72} from $<\text{DL}$ to 0.69 nM (Figure 1g). This corresponds to a percentage of iron dissolved in seawater from total iron introduced ranging from $<\text{DL}$ to 0.0150 %. $\Delta[\text{dFe}]$ at T_{72} was on average 2.6 ± 0.7 times higher than at T_{24} . From December to February, dissolution remained undetectable whatever the contact time considered. Dissolution values increased from April to July, followed by lower but significant values between August and October. Dissolution values at T_{24} and T_{72} as a percentage of apparent free ligands (as measured by CSV) that complexed iron (Figure 1f) were ranging from $<\text{DL}$ to *ca.* 15%.

3.3. Dissolution Kinetics Study (Second Experiment)

[13] The difference between both replicates for $\Delta[\text{dFe}]$ versus time was not significant (t-test, $n = 15$, $p < 0.05$). This good reproducibility supports that the variability of the dissolution evidenced from the first experiment was due to an environmental factor rather than an intra-experimental issue. We attempted to use simple functions (log, exponential, power law, linear) to fit the whole data set, by minimizing the χ^2 differences between model function and experimental points. None of these simple functions were satisfactory and a better and significant fit ($p < 0.0001$) was obtained by adjusting the distribution for the two segments with linear models with a change in the slopes at time $t = 2.6$ hours (Figure 2). The first and second linear segment corresponds respectively to dissolution rates of $1.23 \text{ nM}\cdot\text{Fe}\cdot\text{day}^{-1}$ and $0.09 \text{ nM}\cdot\text{Fe}\cdot\text{day}^{-1}$.

4. Discussion

4.1. Temporal Variation of Iron Binding Ligand Concentrations

[14] The monthly variations of most of the variables measured at 10 m-depth (Figure 1), follow the trends described in previous studies conducted at DYFAMED: [dFe] [Bonnet and Guieu, 2006], TChla [Marty *et al.*, 2002], BA [Lemée *et al.*, 2002] and DOC [Avril, 2002]. The only existing [L'] values in the western Mediterranean Sea are from a cruise that took place in July 1993 [Van den Berg, 1995], where [L_T] (Total iron binding ligands) values at 20 m ($4.2\text{--}5.85 \text{ nM}\cdot\text{eqFe}$) were of the same order of magnitude as the July value in our study ($4.9 \text{ nM}\cdot\text{eqFe}$). Seasonal variations of organic speciation have been demonstrated for copper [Croot, 2003] but, to our knowledge,

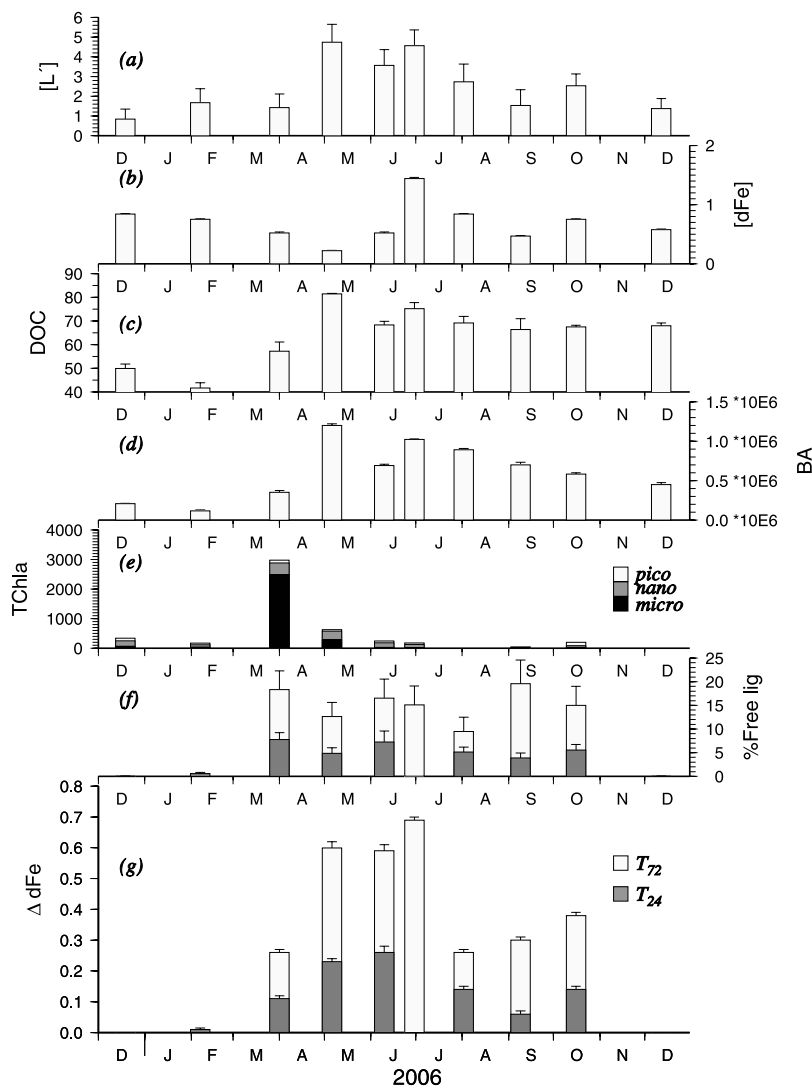


Figure 1. Seasonal variations at 10 m between December 2005 and December 2006 at DYFAMED station of (a) $[L']$ in $\text{nmol.L}^{-1}\text{-Fe}$ equivalent, (b) $[\text{dFe}]$ in nmol.L^{-1} , (c) DOC in $\mu\text{mol.L}^{-1}\text{-C}$ equivalent, (d) BA in cells.mL^{-1} , (e) TChla in ng.L^{-1} for micro-, nano- and pico-phytoplankton (data obtained in the frame of the Service d'Observation DYFAMED—Importance of the different size groups of phytoplankton following the method described by Uitz *et al.* [2006]), (f) percentage of apparent free ligands (as measured by CSV) that complexed iron at T_{24} and T_{72} and (g) $\Delta[\text{dFe}]$ (in nM) dissolved from the particles ($\Delta[\text{dFe}] = [\text{dFe}]_{T_x} - [\text{dFe}]_{T_0}$) at T_{24} (grey bar) and T_{72} (white bar) in nM. The bars are not stacked. The error bars represent the standard deviation for replicate analysis. Corresponding data available in the auxiliary material.

this is the first report of the temporal variability of iron binding ligands at a yearly scale. Different biogenic sources for iron binding ligands have been proposed [Hutchins *et al.*, 1999]: (1) synthesis and release by prokaryotic organisms in iron limited environments and (2) breakdown of biological material. In the present study, variation in ligand concentration presents a significant positive correlation with BA ($r^2 = 0.73$, $p = 0.008$, $n = 10$) and DOC ($r^2 = 0.57$, $p = 0.01$, $n = 10$) whereas no significant correlation is observed with TChla or any phytoplankton group. The two maximum values of $[L']$ (May and July) coincide with peaks in BA: one was observed after the spring bloom (in May), probably fuelled by the high post-bloom DOC pool; the other one, observed in July was likely induced by a Saharan dust event recorded 4 days before [Pulido-Villena *et al.*, 2008].

4.2. Atmospheric Iron Dissolution

[15] The low dissolution percentages obtained in this study are probably due to the use of a Saharan dust end-member composed of terrigenous particles not submitted to atmospheric transport/aging. Our numbers are in agreement with previous studies by Bonnet and Guieu [2004] and Mendez *et al.* [2008] conducted with the same dust.

[16] $\Delta[\text{dFe}]$ increased significantly with $[L']$ and DOC with a constant percentage of free ligands apparently used to complex iron (Figure 1f). Although the final iron concentration is expected to be controlled by iron binding ligands, $\Delta[\text{dFe}]$ is not better correlated to $[L']$ than to DOC (Figures 3a and 3b). These results are in agreement with the theoretical approach introduced by Hiemstra and van Riemsdijk [2006]: the dissolution may not only be seen

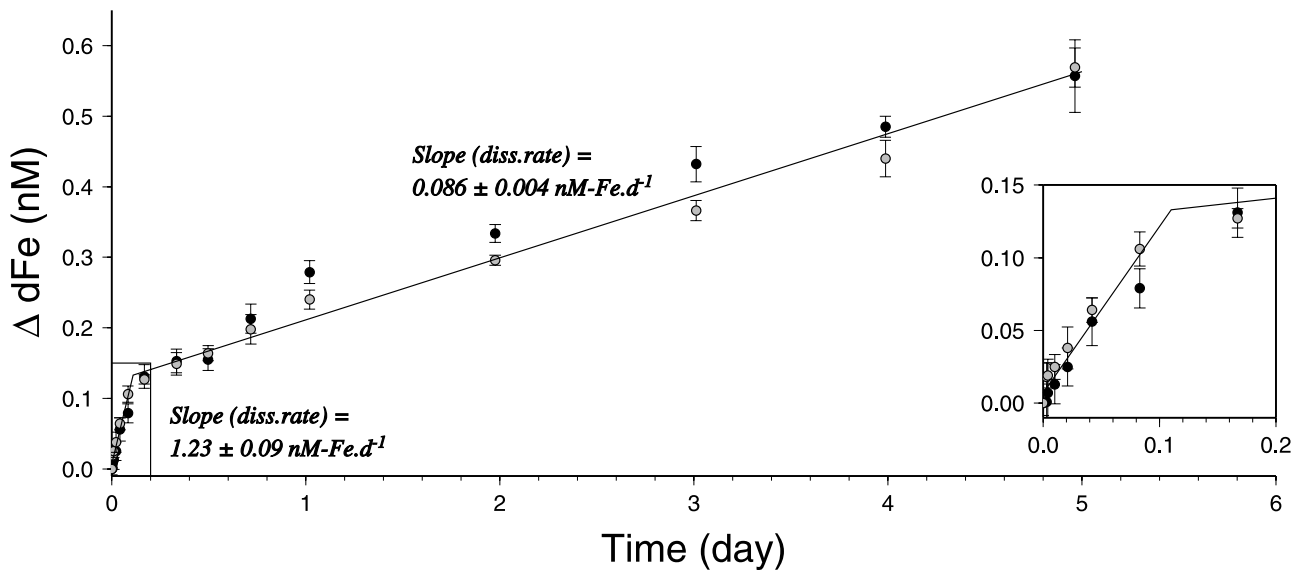


Figure 2. Δ [dFe] (in nM) as a function of time (in day). The grey circles represent the replicate 1 and the black circles, the replicate 2.

as controlled by one (or two) class of organic binding ligands measured by CL-ACSV, but rather by the entire DOM pool which represents a continuum of binding characteristics which could act on dissolution. The obtained dissolution amounts can be classified in three groups

(Figures 3a and 3b), corresponding to contrasting situations regarding biogeochemical conditions. Group (H), where the dissolution is the highest, corresponds to periods when abundance of heterotrophic bacteria is stimulated (end of the bloom or after a dust event). Group (M), with a lower

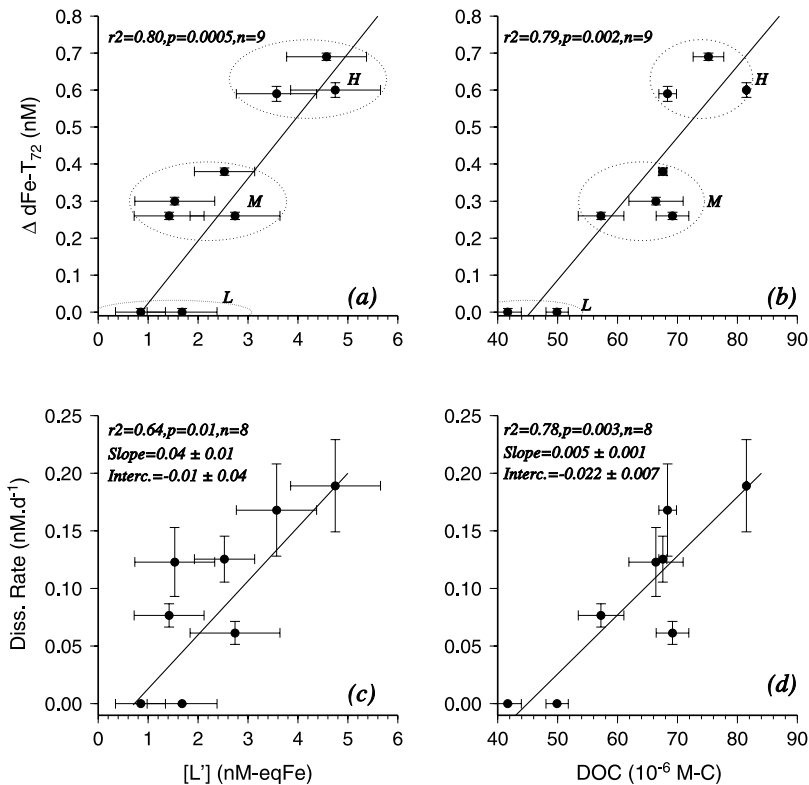


Figure 3. Δ [dFe] (in nM) at T_{72} plotted against (a) $[L']$ and (b) DOC. Dissolution rate between T_{24} and T_{72} plotted against (c) $[L']$ and (d) DOC. For all plots, the point corresponding to “Dec. 06” has been removed due to peculiar hydrological conditions encountered during this month (J. C. Marty and J. Chiaverini, Drastic changes in hydrology and productivity observed in the north-western Mediterranean Sea during 1995–2007 period at DYFAMED time-series station, manuscript in preparation, 2008). The meaning of the data groups *L*, *M* and *H* are explained in the text.

dissolution, corresponds to situations during which the bacterial activity is moderate (during the bloom and when stratification is well established in summer). Finally, group (L) corresponds to the period of winter mixing with low productivity and low bacterial activity when no dissolution could be measured. An intriguing point for this group (L) is that no dissolution is detectable although $[L^I]$ and DOC are still measurable. Contrary to the theoretical approach proposed by *Hiemstra and van Riemsdijk* [2006], it seems necessary to invoke a qualitative description of iron binding ligands to fully understand their effect on iron solubility in seawater. This suggests that the organic matter present in the seawater at that time is not able to dissolve or keep in solution iron from the dust sample used in this study. Organic matter supplied by deep water mixing (during winter months) could be seen in a conceptual way as “old” degradation products which would be “non effective” to hold iron in solution. In contrast, periods with high dissolution would correspond to conditions of “freshly” produced organic matter as illustrated in this time-series by the higher dissolution values encountered in May and July. This can be compared to $[dFe]$ and $[L^I]$ patterns observed during *SOIREE* iron enrichment [*Croot et al.*, 2001] where the post infusion $[dFe]$ increased only when “new” ligands were produced.

4.3. Dissolution Kinetics

[17] In the second experiment, iron dissolution kinetics can be modeled by two linear functions. This approach is insufficient to give a mechanistic description of a ligand induced dissolution of dust iron. However, these two dissolution rates imply that a fraction of iron within the dust particles is more easily prone to dissolve since the first slope corresponds to a dissolution rate ten times higher than the second one. When all the “easily” dissolvable iron is released, the dissolution rate decreases down to $0.09 \text{ nM} \cdot \text{day}^{-1}$. The first slope could consist of the addition of this slower rate and a faster rate of dissolution of $1.14 \text{ nM} \cdot \text{Day}^{-1}$. This idea of two different “types” of iron in regard to the solubility is in agreement with previous studies that have demonstrated that iron solubility depends on the different solid phases (clays, iron oxides, quartz) that constitute dust particles [*Journet et al.*, 2008]. No decrease of the dissolution rate at the end of the experiment could be observed, but we can suppose that this would occur when the binding equilibrium between the available ligands and iron would be reached [*Liu and Millero*, 2002]. This point is clearly not yet reached as the $[dFe]$ at the end of the experiment is equal to $0.77 \pm 0.05 \text{ nM}$ ($n = 2$) whereas $[L^I]$ is 2.54 nM-eqFe at the beginning of the experiment.

[18] Since the dissolution kinetics observed in the second experiment (“slow” dissolution after 4 hours) may certainly apply to the first experiment, we can assume that dissolution occurred linearly between T_{24} and T_{72} . Thus, for all seawater used in the first experiment, we can estimate the dissolution rate of iron from the slope of the line defined between $\Delta[dFe]$ at T_{24} and at T_{72} . This dissolution rate is linearly dependent on the $[L^I]$ and DOC (Figures 3c and 3d). This control of the dissolution kinetics by DOM is also supported by the fact that the amount of dissolved iron represents a relatively constant fraction of the available binding ligands for all the months in the first experiment

(Figure 1e). Since DOC is a parameter widely determined in the ocean, such a linear model between the dissolution rate and DOC could be of great interest for studies at the global scale. However, the role of aerosol properties and atmospheric transport toward dissolution needs also to be taken into account in order to thoroughly parameterize the dissolution of atmospheric iron in seawater.

5. Conclusion

[19] So far, it has been demonstrated experimentally that iron-binding ligands affect iron dissolution rates when siderophore ligands, artificial [*Kraemer*, 2004] or from natural bacterial cultures [*Yoshida et al.*, 2002], are added to pure iron (hydr)oxides. Here, in natural conditions, we show that this applies to the dissolution of iron from dust particles when they enter the sea surface. Over a one year time series, the ultimate control of atmospheric iron dissolution by iron binding ligands [*Liu and Millero*, 2002; *Mendez et al.*, 2008] is confirmed. However, in this study, iron binding ligands concentration as determined by CL-ACSV is not a better parameter than DOC to parameterize this process. In regard to the importance of organic complexation in the dissolution process demonstrated in this study, investigating the influence of light seems a promising perspective, due to the importance of the light induced processes on organically-bound iron bioavailability [*Barbeau et al.*, 2001]. Since, the trophic conditions control the concentration of dissolved organic matter in the surface ocean, and given the fertilizing potential of atmospheric iron, dissolved organic matter may certainly mediate a positive feedback between dust and ocean biogeochemistry.

[20] **Acknowledgments.** We thank the crew of the R/V *Théthys II*. S. Blain, S. Bonnet, P. Ludgate and three anonymous reviewers are acknowledged for their very helpful comments. This work was supported by INSU, CNRS and the ANR funded program BOA (PI: Géraldine Sarthou and Karine Desboeufs). A BDI grant of the Region PACA and CNRS supported T.W.

References

- Avril, B. (2002), DOC dynamics in the northwestern Mediterranean Sea (DYFAMED site), *Deep Sea Res., Part II*, 49, 2163–2182.
- Baker, A. R., and T. D. Jickells (2006), Mineral particle size as a control on aerosol iron solubility, *Geophys. Res. Lett.*, 33, L17608, doi:10.1029/2006GL026557.
- Barbeau, K., E. L. Rue, K. W. Bruland, and A. Butler (2001), Photochemical cycling of iron in the surface ocean mediated by microbial iron (III)-binding ligands, *Nature*, 413, 409–413.
- Bonnet, S., and C. Guieu (2004), Dissolution of atmospheric iron in seawater, *Geophys. Res. Lett.*, 31, L03303, doi:10.1029/2003GL018423.
- Bonnet, S., and C. Guieu (2006), Atmospheric forcing on the annual iron cycle in the western Mediterranean Sea: A 1-year survey, *J. Geophys. Res.*, 111, C09010, doi:10.1029/2005JC003213.
- Croot, P. L. (2003), Seasonal cycle of copper speciation in Gullmar Fjord, Sweden, *Limnol. Oceanogr.*, 48(2), 764–776.
- Croot, P. L., and M. Johansson (2000), Determination of iron speciation by cathodic stripping voltammetry in seawater using the competing ligand 2-(2-thiazolylazo)-*p*-cresol (TAC), *Electroanalysis*, 12, 565–576.
- Croot, P. L., A. R. Bowie, R. D. Frew, M. T. Maldonado, J. A. Hall, K. A. Safi, J. La Roche, P. W. Boyd, and C. S. Law (2001), Retention of dissolved iron and Fe^{II} in an iron induced Southern Ocean phytoplankton bloom, *Geophys. Res. Lett.*, 28(18), 3425–3428, doi:10.1029/2001GL013023.
- Fischer, A., J. Kroon, T. Verburg, T. Teunissen, and T. H. Wolterbeek (2007), On the relevance of iron adsorption to container materials in small-volume experiments on iron marine chemistry: ^{55}Fe -aided assessment of capacity, affinity and kinetics, *Mar. Chem.*, 107, 533–546.
- Guieu, C., M.-D. Loye-Pilot, C. Ridame, and C. Thomas (2002), Chemical characterization of the Saharan dust end-member: Some biogeochemical

- implications for the western Mediterranean Sea, *J. Geophys. Res.*, *107*(D15), 4258, doi:10.1029/2001JD000582.
- Hiemstra, T., and W. H. van Riemsdijk (2006), Biogeochemical speciation of Fe in ocean water, *Mar. Chem.*, *102*, 181–197.
- Hutchins, D. A., A. E. Witter, A. Butler, and G. W. Luther (1999), Competition among marine phytoplankton for different chelated iron species, *Nature*, *400*, 858–861, doi:10.1038/23680.
- Journet, E., K. V. Desboeufs, S. Caquineau, and J.-L. Colin (2008), Mineralogy as a critical factor of dust iron solubility, *Geophys. Res. Lett.*, *35*, L07805, doi:10.1029/2007GL031589.
- Kraemer, S. (2004), Iron oxide dissolution and solubility in the presence of siderophores, *Aquat. Sci.*, *66*, 3–18.
- Lemée, R., E. Rochelle-Newall, F. Van Wambeke, M. D. Pizay, P. Rinaldi, and J. P. Gattuso (2002), Seasonal variation of bacterial production, respiration and growth efficiency in the open NW Mediterranean Sea, *Aquat. Microb. Ecol.*, *29*, 227–237.
- Liu, X. W., and F. J. Millero (2002), The solubility of iron in seawater, *Mar. Chem.*, *77*, 43–54.
- Martin, J. H. (1990), Glacial-interglacial CO₂ change: The iron hypothesis, *Paleoceanography*, *5*, 1–13.
- Marty, J. C., J. Chiaverini, M. D. Pizay, and B. Avril (2002), Seasonal and interannual dynamics of nutrients and phytoplankton pigments in the western Mediterranean Sea at the DYFAMED time-series station (1991–1999), *Deep Sea Res., Part II*, *49*, 1965–1985.
- Mendez, J., et al. (2008), Atmospheric input of manganese and iron to the ocean: Seawater dissolution experiments with Saharan and North American dusts, *Mar. Chem.*, in press.
- Pulido-Villena, E., T. Wagener, and C. Guieu (2008), Bacterial response to dust pulses in the western Mediterranean: Implications for carbon cycling in the oligotrophic ocean, *Global Biogeochem. Cycles*, *22*, GB1020, doi:10.1029/2007GB003091.
- Sedwick, P. N., E. R. Sholkovitz, and T. M. Church (2007), Impact of anthropogenic combustion emissions on the fractional solubility of aerosol iron: Evidence from the Sargasso Sea, *Geochem. Geophys. Geosyst.*, *8*, Q10Q06, doi:10.1029/2007GC001586.
- Uitz, J., H. Claustre, A. Morel, and S. B. Hooker (2006), Vertical distribution of phytoplankton communities in open ocean: An assessment based on surface chlorophyll, *J. Geophys. Res.*, *111*, C08005, doi:10.1029/2005JC003207.
- Van den Berg, C. M. G. (1995), Evidence for organic complexation of iron in seawater, *Mar. Chem.*, *50*, 139–157.
- Yoshida, T., K. Hayashi, and H. Ohmoto (2002), Dissolution of iron hydroxides by marine bacterial siderophore, *Chem. Geol.*, *184*, 1–9.

C. Guieu, E. Pulido-Villena, and T. Wagener, Laboratoire d’océanographie de Villefranche, UMR7093, CNRS, Caserne Nicolas, Quai de la Darse, F-06238 Villefranche-sur-Mer, France. (wagener@ovs-vlfr.fr)